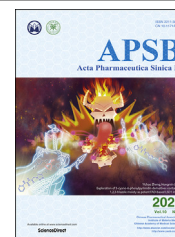




Chinese Pharmaceutical Association
Institute of Materia Medica, Chinese Academy of Medical Sciences

Acta Pharmaceutica Sinica B

www.elsevier.com/locate/apsb
www.sciencedirect.com



ORIGINAL ARTICLE

Deficiency of anti-inflammatory cytokine IL-4 leads to neural hyperexcitability and aggravates cerebral ischemia–reperfusion injury



Xiaoling Chen^{a,†}, Jingliang Zhang^{a,†}, Yan Song^a, Pan Yang^b,
Yang Yang^c, Zhuo Huang^a, Kewei Wang^{a,b,d,*}

^aDepartment of Molecular and Cellular Pharmacology, State Key Laboratory of Natural and Biomimetic Drugs, Peking University School of Pharmaceutical Sciences, Beijing 100191, China

^bDepartment of Pharmacology, Qingdao University School of Pharmacy, Qingdao 266021, China

^cDepartment of Medicinal Chemistry and Molecular Pharmacology, Purdue University College of Pharmacy, West Lafayette, IN 47907, USA

^dInstitute of Innovative Drugs, Qingdao University School of Pharmacy, Qingdao 266021, China

Received 5 January 2020; received in revised form 21 February 2020; accepted 9 March 2020

KEY WORDS

Anoxic depolarization;
IL-4;
Ischemia–reperfusion
injury;
Neuronal excitability;
Synaptic transmissions

Abstract Systematic administration of anti-inflammatory cytokine interleukin 4 (IL-4) has been shown to improve recovery after cerebral ischemic stroke. However, whether IL-4 affects neuronal excitability and how IL-4 improves ischemic injury remain largely unknown. Here we report the neuroprotective role of endogenous IL-4 in focal cerebral ischemia–reperfusion (I/R) injury. In multi-electrode array (MEA) recordings, IL-4 reduces spontaneous firings and network activities of mouse primary cortical neurons. IL-4 mRNA and protein expressions are upregulated after I/R injury. Genetic deletion of *Il-4* gene aggravates I/R injury *in vivo* and exacerbates oxygen-glucose deprivation (OGD) injury in cortical neurons. Conversely, supplemental IL-4 protects *Il-4*^{-/-} cortical neurons against OGD injury. Mechanistically, cortical pyramidal and stellate neurons common for ischemic penumbra after I/R injury exhibit intrinsic hyperexcitability and enhanced excitatory synaptic transmissions in *Il-4*^{-/-} mice. Furthermore, upregulation of Nav1.1 channel, and downregulations of KCa3.1 channel and $\alpha 6$ subunit of GABA_A receptors are detected in the cortical tissues and primary cortical neurons from *Il-4*^{-/-} mice. Taken together, our find-

*Corresponding author. Tel.: +86 532 82991070.

E-mail addresses: wangkw@qdu.edu.cn, wangkw@bjmu.edu.cn (Kewei Wang).

[†]These authors made equal contributions to this work.

Peer review under the responsibility of Chinese Pharmaceutical Association and Institute of Materia Medica, Chinese Academy of Medical Sciences.

<https://doi.org/10.1016/j.apsb.2020.05.002>

2211-3835 © 2020 Chinese Pharmaceutical Association and Institute of Materia Medica, Chinese Academy of Medical Sciences. Production and hosting by Elsevier B.V. This is an open access article under the CC BY-NC-ND license (<http://creativecommons.org/licenses/by-nc-nd/4.0/>).

ings demonstrate that IL-4 deficiency results in neural hyperexcitability and aggravates I/R injury, thus activation of IL-4 signaling may protect the brain against the development of permanent damage and help recover from ischemic injury after stroke.

© 2020 Chinese Pharmaceutical Association and Institute of Materia Medica, Chinese Academy of Medical Sciences. Production and hosting by Elsevier B.V. This is an open access article under the CC BY-NC-ND license (<http://creativecommons.org/licenses/by-nc-nd/4.0/>).

1. Introduction

Stroke is the second leading cause of death and the major cause of long-term disability worldwide. Ischemic stroke represents approximately 87% of all brain strokes¹. During ischemic stroke, energy depletion induces anoxic depolarization and excitotoxicity of cortical neurons characterized by progressive cell death and development of permanent local brain damage². Meanwhile, proinflammatory mediators are released from activated resident microglia for participation in neuroinflammation³, further aggravating neuronal loss and brain damage.

Conversely, several lines of evidence suggest that neurons can rapidly respond to ischemic conditions by secreting molecules that support brain tissue healing and repairing^{4,5}. It has recently been shown that as an intrinsic defense mechanism neurons produce and secrete anti-inflammatory cytokine interleukin 4 (IL-4) in response to sublethal ischemic injury⁶. IL-4 participates in protecting injured neurons in central nervous system⁷. Interleukin 4 receptor alpha chain (IL-4R α) is expressed in neurons and plays a critical role in modulating neuronal death through activation of signal transducer and activator of transcription 6 (STAT6) during ischemia⁸. IL-4 stimulates microglial phagocytosis and enables efficient clearance of apoptotic neurons for repair⁶. Systemic administration of IL-4 also reduces ischemic lesion and improves neurologic function after stroke^{6,9–11}. All these investigations indicate that neuronal IL-4 is actively involved in promoting recovery of brain injury after stroke. However, the underlying mechanism for neuroprotective role of neuronal IL-4 in ischemic recovery remains largely unknown.

Previous studies have shown that the anti-apoptotic function of IL-4 is closely related to hyperpolarization of mitochondrial membrane potential in different cells including effector CD4 cells¹² and B cells¹³. The interaction of IL-4 with its high-affinity receptor IL-4R α and the subsequent recruitment of the IL-2R γ chain^{14,15} are related to membrane depolarization of T cells¹⁶. The upregulation of IL-4 expression influences membrane potential oscillations due to opening of intermediate/small conductance calcium-activated K⁺ channel (KCa3.1, encoded by *Kcnn4* gene) in macrophages¹⁷. Interestingly, IL-4 upregulates KCa3.1 expression and increases KCa3.1 current through IL-4 receptor (IL-4R) signaling pathway in microglia¹⁸, and KCa3.1 contributes to regulation of after-hyperpolarization potentials (AHPs)¹⁹. All these investigations suggest that an enhanced neuronal IL-4 signaling may regulate neuronal membrane potential, thus affecting the excitability of neurons in the brain. We, therefore, hypothesize that neuronal IL-4 might have a direct impact on anoxic depolarization or hyperexcitability during ischemic injury after stroke.

To test this hypothesis, we utilized *Il-4* knockout (KO) mice and found that *Il-4*^{-/-} mice were more susceptible to

ischemia–reperfusion (I/R) injury induced by transient middle cerebral artery occlusion (tMCAO) *in vivo*, and neurons from *Il-4*^{-/-} mice were hyperexcitable. Mechanistically, genetic deletion of *Il-4* resulted in intrinsic hyperexcitability in cortical neurons with upregulation of Nav1.1 channels, and downregulations of KCa3.1 channels and $\alpha 6$ subunits of GABA_A receptors. These findings for the first time demonstrate a previously unknown mechanism that loss of IL-4 causes neural hyperexcitability, and the enhancement of neuronal IL-4 signaling by reduction of neuronal firing can protect the brain against development of permanent damage and help recover from ischemic injury after stroke.

2. Materials and methods

2.1. Chemicals and agents

NMDA receptor antagonist D-2-amino-5-phosphonovalerate (AP5) and α -amino-3-hydroxy-5-methyl-4-isoxazole-propionate (AMPA)/kainate glutamate receptor antagonist 6-cyano-7-nitroquinoxaline-2,3-dione (CNQX) were obtained from Sigma (St. Louis, MO, USA). GABA_A receptor antagonist bicuculline was purchased from Abcam (Cambridge, UK). NeurobiotinTM tracer *N*-(2-aminoethyl) biotinamide hydrochloride was purchased from Vector Laboratories (Burlingame, CA, USA), and molecular probe Alexa 488-conjugated streptavidin was obtained from Invitrogen (Carlsbad, CA, USA). Neuronal medium NbActiv4 was from Brain Bits (Springfield, IL, USA), animal-free murine IL-4 was purchased from Peprotech (Rocky Hill, NJ, USA).

2.2. *Il-4* gene knockout mice

A “*neo cassette*” was inserted into the SacI site (GAGCTC) in the exon 3 of the interleukin 4 gene (ID: 16189) to produce the *Il-4* gene KO mice (Supporting Information Fig. S2A). The genotyping was determined using polymerase chain reaction (PCR). Briefly, genomic DNA was extracted from ear or tail (0.2 cm) using the alkali extraction method²⁰. A PCR was then performed using Ex Taq polymerase (TaKaRa-Bio, Kusatsu, Japan) and the following primers: primer 1, 5'-GTTGAGCAGATGACATTGGG GC-3'; primer 2, 5'-CTTCAAGCATGGAGTTTCCCC-3'; primer 3, 5'-GCGCATCGCCTTCTATCGCCTTC-3'.

The PCR consisted of an initial 2 min at 94 °C, followed by 40 cycles of 15 s at 94 °C, 30 s at 57 °C and 30 s at 72 °C. After the last cycle, the reaction is kept at 72 °C for 10 min before held at 4 °C. A 180 bp cDNA band was observed for wild-type allele, whereas a 208 bp band was detected for the mutant allele, and heterozygotes containing both alleles were detected with the two bands.

2.3. Multi-electrode array (MEA) recordings

Cortical neurons from newborn C57BL/6J mice (<24 h) were acutely dissociated and suspended in NbActiv4 (Brain Bits) medium. Approximately $\sim 7 \times 10^4$ neurons in 8 μL medium were seeded on 12-well MEA plates (Axion Biosystems Inc, Atlanta, GA, USA) coated with poly-D-lysine (40 $\mu\text{g}/\text{mL}$)/laminin (20 $\mu\text{g}/\text{mL}$). 20 ng/mL IL-4 (Peprotech) was added in the culture media in IL-4 group for 16 days. On the 3rd day, cytarabine (2.5 $\mu\text{g}/\text{mL}$) was added to suppress the proliferation of glial cells by mitotic inhibition for up to seven days²¹.

Neuronal activities were recorded using an MEA system (Axion Maestro Pro) and data are analyzed using Axion Integrated Studio AxIS2.1 (Axion Biosystems Inc, Atlanta, GA, USA) and NeuroExplorer (Nex Technologies, Madison, AL, USA) as previously described²². In the MEA recordings, a spike detection criterion of >6 standard deviations above the background was used to separate monophasic or biphasic action potential spikes from the noise²². Active electrodes were defined as >1 spike over a 200-s analysis period. Firing frequencies were averaged among all active electrodes from wells expressing either construct²².

2.4. Whole-cell patch clamp recordings of acute brain slices

Mice were anesthetized with pentobarbital sodium (60 mg/kg, i.p.) and decapitated before their brains were dissected into ice-cold slicing solution. Acute horizontal (for patch recordings of medial entorhinal cortex (mEC) layer II stellate neurons) or coronal slices (for patch recordings of motor cortical neurons) at a 300- μm thickness on a vibratome (Leica VT1200S, Leica, Nussloch, Germany) and transferred to normal artificial cerebrospinal fluid (ACSF). Then, slices were incubated at 37 °C for 20–30 min and stored at room temperature before use.

The medium after-hyperpolarization potential (mAHP) slope was calculated with Eq. (1):

$$\text{mAHP slope (mV/ms)} = (V_{\text{small-peak}} - V_{\text{trough}}) / (T_{\text{small-peak}} - T_{\text{trough}}) \quad (1)$$

where $V_{\text{small-peak}}$ and $T_{\text{small-peak}}$ are the small peak membrane potential and time-point at the end of an action potential (AP) respectively, V_{trough} and T_{trough} are the trough membrane potential and time-point at the end of fast after-hyperpolarization potential (fAHP), respectively.

The sag ratio was calculated with Eq. (2):

$$\text{Sag ratio} = (V_{\text{baseline}} - V_{\text{steady-state}}) / (V_{\text{baseline}} - V_{\text{min}}) \quad (2)$$

where V_{baseline} is the resting membrane potential or -70 mV, V_{min} is the minimum voltage reached soon after the hyperpolarizing current pulse, and $V_{\text{steady-state}}$ is the average voltage recorded at 0–10 ms before the end of the -200 pA stimulus.

The input resistance (IR) was calculated with Eq. (3):

$$\text{Input resistance (M}\Omega) = (V_{\text{baseline}} - V_{\text{steady-state}}) \times 10 \quad (3)$$

where V_{baseline} is the resting membrane potential or -70 mV, and $V_{\text{steady-state}}$ is the average voltage recorded at 0–10 ms before the end of the -100 pA stimulus.

For whole-cell voltage-clamp recordings of miniature inhibitory postsynaptic currents (mIPSCs), the internal solution contained (in mmol/L): 122 CsCl, 1 CaCl₂, 5 MgCl₂, 10 EGTA, 10 HEPES, 4 Na₂ATP, 0.3 Tris-GTP, 14 Tris-phosphocreatine, adjusted to pH 7.3 with CsOH. Tetrodotoxin (TTX; sodium

channel blocker, 0.5 $\mu\text{mol}/\text{L}$), AP5 (NMDA receptor antagonist, 50 $\mu\text{mol}/\text{L}$), CNQX (AMPA/kainate glutamate receptor antagonist, 10 $\mu\text{mol}/\text{L}$) were applied to block excitatory synaptic transmission. For recordings of miniature excitatory postsynaptic currents (mEPSCs), the internal solution contained (in mmol/L): 118 KMeSO₄, 15 KCl, 2 MgCl₂, 0.2 EGTA, 10 HEPES, 4 Na₂ATP, 0.3 Tris-GTP, 14 Tris-phosphocreatine, adjusted to pH 7.3 with KOH. TTX, bicuculline (GABA_A receptor antagonist, 10 $\mu\text{mol}/\text{L}$) and CGP55845 (selective GABA_B receptor antagonist, 2 $\mu\text{mol}/\text{L}$) were applied to block inhibitory synaptic transmission. We used thick-wall borosilicate glass pipettes, which were pulled with open-tip resistances of 4–6 M Ω . Slices were maintained under continuous perfusion of ACSF at 32–33 °C with a flow rate of 2–3 mL/min. In the whole-cell configuration, series resistance (R_s) was maintained at the range of 15–30 M Ω , and the recordings with unstable R_s or a change of $R_s > 20\%$ were aborted.

For cell labeling, the internal solution either for whole-cell current clamp recordings or for voltage-clamp recordings contained 0.1%–0.2% (w/v) neurobiotin tracer. At the end of the electrophysiological recordings (~ 30 min), slices were treated as previously described^{23,24}. Labeled neurons in brain slices were imaged by laser scanning confocal microscopy (TCS-SP8 STED 3X, Leica Microsystems, Wetzlar, Germany) with 40 \times oil-immersion objectives for pyramidal neurons and 63 \times oil-immersion objectives for stellate neurons.

All recordings were performed at least 10 min after breakthrough for internal solution exchange equilibrium using a MultiClamp 700B amplifier (Molecular Device, Sunnyvale, CA, USA), and data were acquired using pCLAMP 10.6 software and filtered using a Digidata 1440A digitizer (Molecular Devices, Sunnyvale, CA, USA). Only a single neuron was recorded in each brain slice.

2.5. Culture of mouse primary cortical neurons

Cortical neurons were dissociated from newborn mice (within 24 h) by 0.25% trypsinization²⁵. Cells were suspended in high-glucose DMEM (Gibco, Gaithersburg, MD, USA) containing 10% fetal bovine serum (Gibco) before plated on poly-D-lysine hydrobromide (Sigma–Aldrich) coated 12-well culture plates at a density of approximate 1.2×10^5 cells/cm² for different experiments. After 4–6 h seeding, the medium was changed to phenol red-free neurobasal A medium (Gibco) supplemented with 2% B27 (Gibco), containing 0.5 mmol/L GlutaMAX-I, and 0.5% penicillin–streptomycin before one-half medium was refreshed every three days. On the 3rd day, cytarabine (2.5 $\mu\text{g}/\text{mL}$) was added to suppress the proliferation of glial cells by mitotic inhibition for up to seven days²¹. Cells were maintained at 37 °C in a humidified atmosphere containing 95% air and 5% CO₂ and used for experiments after 7–9 days *in vitro*.

2.6. In vivo model of I/R injury induced by middle cerebral artery occlusion in mice

C57BL/6J mice (12 ± 2 weeks) were obtained from the Department of Laboratory Animal Science, Peking University Health Science Center (Beijing, China). The *Il-4* gene knockout mice (12 ± 2 weeks, background is C57BL/6J) were kindly provided by Kopf's group²⁶ and bred in our animal facility. All experimental procedures were approved by the Beijing Committee for Animal Care and Use. The surgery protocol was approved by the

Committee on the Ethics of Animal Experiments of Peking University Health Science Center (Beijing, China).

Mice were anesthetized with pentobarbital sodium (60 mg/kg, i.p.). A probe was connected to the left skull for monitoring relative local cerebral blood flow (LCBF) with laser Doppler flowmetry (LDF) (Periflux 5000, Perimed, Sweden). Transient focal cerebral ischemia was induced by left tMCAO for 90 min. The LCBF drops and maintains below 80% of the baseline during ischemia²⁷. Scoring of neurological deficits following stroke was evaluated by the Longa method according to an expanded 7 scale²⁸. The observer was blind to animal treatment, and one mouse obtaining no less than 2 scores was counted as a valid model. Infarct areas were analyzed using Adobe Photoshop CC and determined by an indirect method correcting for edema²⁹.

2.7. Oxygen-glucose deprivation (OGD) injury in mouse cortical neurons

The *in vitro* OGD injury model was generated as previously described³⁰. The original media were replaced with a glucose-free and phenol red-free DMEM containing 10 mmol/L of sodium dithionite (Na₂S₂O₄), a deoxygenated reagent for 30 min (or 20 min), before return to their original culture medium for maintenance of 24 h until the assay of cell injury.

The release amount of lactate dehydrogenase (LDH) into the culture medium as a measurement of cell death was measured using LDH assay reagent (Promega, Fitchburg, WI, USA) according to the instructions³⁰. The survival cell viability was estimated by a cell counting kit-8 assay (CCK-8, Dojindo, Kumamoto, Japan)³¹. At least three wells were measured in each group. For the calculation of LDH release, we took the value in the sham group as 100%, and the value in the OGD group was divided by the sham group to get the relative value of LDH release. In the rescue experiment, we took the *IL-4*^{-/-} group value as 100%, and the value of adding IL-4 was divided by that of *IL-4*^{-/-} group to get the relative value.

2.8. RNA isolation, reverse transcription and qRT-PCR analysis

After MCAO surgery for 6, 12, and 24 h, the brains were divided ischemia part and contralateral part to extract RNAs. Total RNAs were extracted with TRIzol reagent (Sigma) from mouse cerebral tissues or cortical neurons according to the manufacturer's instructions. 4 µg RNA was subjected to reverse transcription (RT) with a GoScript™ Reverse Transcription System (Promega), and the resulting cDNA subjected to quantitative RT-PCR analysis with the use of GoTaq[®] qPCR Master Mix (Promega) and specific primers in a 7500 Fast Real-Time PCR System (Applied Biosystems). PCR primer sequences were listed in the Supporting Information Table S7. The calculation was based on follows using the $\Delta\Delta C_t$ method³². For calculation of relative expression of *IL-4* mRNAs in each brain after ischemic injury, we took the contralateral value as 1, and the ischemic area part value was divided by the value from the contralateral part to get the relative value.

2.9. Western blot

After MCAO surgery for 6, 12, and 24 h, mouse brains were removed and divided ischemia part and contralateral part to extract whole protein. Total proteins were extracted in cold RIPA lysis buffer containing 2% cocktail (Roche, Indianapolis, IN, USA). Protein samples were loaded on 10% sodium dodecyl sulfate-

polyacrylamide gel electrophoresis before transferred to PVDF membranes (Millipore Corporation, Bedford, MA, USA). After blocking by 5% milk, PVDF membranes were incubated with primary antibodies at 4 °C overnight such as rat anti-IL-4 antibody (1:500, Abcam, ab11524), mouse monoclonal anti-KCa3.1 antibody (1:250, Alomone, ALM-051), rabbit anti-Nav1.1 antibody (1:250, Alomone, ASC-001), rabbit GABA_A R $\alpha 6$ Polyclonal Antibody (1:200, Alomone, AGA-004), mouse anti- β -actin antibody (1:5000, Abcam) and mouse anti-GAPDH antibody (1:5000, Abcam). The membranes were then incubated with their corresponding secondary horseradish peroxidase-conjugated antibodies before detected using an ECL Western blotting detection system (Millipore). The immunoreactive bands were scanned by Tanon 5200 instrument, captured by Tanon MP system before quantitative analysis by densitometry with Tanon GIS software. For calculation of relative expression of IL-4 proteins, we took the contralateral value as 1, and the ischemic area value was divided by the value from the contralateral part to get the relative value.

2.10. Immunostaining and confocal microscopy

Mouse primary cortical neurons in 15 mm culture dish after seven to nine days were fixed with 4% PFA for 15 min at room temperature after washed three times by 0.01 mol/L PBS before blocked by 10% sheep serum with 0.3% Triton X-100 (Amresco, Solon, OH, USA) in 0.01 mol/L PBS for 1 h. Cells were incubated overnight at 4 °C with primary antibodies including rabbit monoclonal NeuN antibody (1:1000, Abcam, ab177487), mouse monoclonal anti-KCa3.1 antibody (1:200, Alomone, ALM-051) and rabbit anti-Nav1.1 antibody (1:200, Alomone, ASC-001). To test neuronal purity of the primary cultured cortical neurons, we also used rabbit anti-GFAP (glial fibrillary acidic protein) antibody (1:200, Abcam, ab16997) for astrocytes; recombinant anti-Iba1 (ionized calcium-binding adaptor molecule-1) antibody [EPR16589] (1:500, Abcam, ab178847) for microglial cells; and rat mAb to anti-MBP (Myelin basic protein) antibody (1:100, Abcam, ab7349) for oligodendrocytes. The immunoreactivity was visualized with Alexa Fluor 488- or 594-conjugated secondary antibodies (1:500; ZSGB-BIO) and goat anti-rat IgG H&L (Alexa Fluor[®] 488) (1:500, Abcam, ab150165). The nuclei were stained by Hoechst33342. Immunocytochemical staining was scanned by confocal microscopy (TCS SP8 II, Leica Microsystems, Wetzlar, Germany).

2.11. Statistical analysis

All data are expressed as the means \pm SEM. Unless otherwise noted, statistical significance was determined using unpaired Student's *t*-test for comparison between two groups. Two-way ANOVA with Bonferroni's multiple comparisons test was used for the comparison between multiple groups. Each "n" indicates the number of independent experiments. A value of *P* < 0.05 was considered to be statistically significant.

3. Results

3.1. Reduction of spontaneous firings and network activities of mouse primary cortical neurons by IL-4 in multi-electrode array recordings

To test whether IL-4 had a direct effect on neuronal firings, we started performing multi-electrode array (MEA) recordings of

spontaneous firings in primary cortical neurons in the presence of cytarabine that inhibits glial cells to purify neurons to 92.0% (Supporting Information Fig. S1). As shown in Fig. 1, robust spontaneous firings of cortical neurons were recorded, and adding IL-4 (20 ng/mL) decreased the spike frequency about 26% (Fig. 1A), burst activity about 36% (Fig. 1B), network bursting frequency about 17% and the synchrony of spontaneous spikes about 22% (Fig. 1C). These data show that IL-4 attenuates spontaneous neuronal firing and network burst activity, suggesting a direct effect of IL-4 on neural excitability.

3.2. Increased neuronal excitability and excitatory synaptic transmissions of cortical neurons in *Il-4*^{-/-} mice

To confirm the effect of IL-4 on neural excitability, we utilized *Il-4* gene knockout (*Il-4*^{-/-}) mice generated by Kopf's group (Supporting Information Fig. S2). As ischemic penumbra after I/R injury commonly occurs in the cortex where IL-4 and IL-4R α are also expressed⁸, we recorded the layer II/III pyramidal neurons in the motor cortex (M1) that controls motor function³³ and layer II stellate neurons in mEC that provides main excitatory inputs to the hippocampus³⁴.

In response to a series of 400 ms current steps, layer II/III pyramidal neurons from *Il-4*^{-/-} mice fired more action potentials (APs) and exhibited depolarized resting membrane potentials (RMPs, Fig. 2A–D and Supporting Information Table S1), indicating that *Il-4*^{-/-} neurons were hyperexcitable mainly due to their depolarized RMPs. When holding at -70 mV, the mAHP slope increased in *Il-4*^{-/-} pyramidal neurons (Supporting Information Fig. S2F).

To further investigate whether *Il-4* null had any influence on synaptic transmissions, we recorded of cortical pyramidal neurons for miniature excitatory postsynaptic currents (mEPSCs) and miniature inhibitory postsynaptic currents (mIPSCs). The mEPSC frequency of *Il-4*^{-/-} pyramidal neurons, but not the mIPSC,

increased with cumulative probability of shorter inter-event intervals (Fig. 2E–G and Supporting Information Tables S2 and S3), indicating that *Il-4*^{-/-} neurons exhibited enhanced excitatory synaptic transmissions.

Current-clamp recordings of *Il-4*^{-/-} stellate neurons further confirmed the increased number of APs due to depolarized RMP (Fig. 2H–K and Supporting Information Table S4), increased mAHP slope at -70 mV (Fig. S2J), and enhanced mEPSC frequency (Fig. 2L–N and Supporting Information Table S5), but not the mIPSC (Supporting Information Table S6), consistent with the observations for the pyramidal neurons. All these results indicated that IL-4 deficiency enhanced neuronal excitability and excitatory synaptic transmissions in both cortical pyramidal and stellate excitatory neurons.

3.3. Upregulation of IL-4 in ischemic brain after focal I/R injury

To examine the expression of IL-4 after brain injury, we generated mouse focal cerebral ischemia by tMCAO for 90 min and reperfusion for different durations (6, 12 and 24 h). As shown in Fig. 3A, the mRNA expression of *Il-4* in the Isc region after tMCAO increased to 3.5-fold at 6 h, 2.4-fold at 12 h and declined to the baseline level at 24 h after reperfusion. Western blot analysis further revealed that the protein expression of IL-4 in the Isc hemisphere increased to 3.0-fold after reperfusion for 24 h (Fig. 3B). These results suggested the upregulation of IL-4 signaling under ischemic conditions.

3.4. Aggravation of focal brain I/R injury by *Il-4* silencing in mice

To examine the role of IL-4 in ischemic injury, both *Il-4*^{-/-} and *Il-4*^{+/+} mice were subjected to tMCAO injury for 90 min as monitored by the decline of local cerebral blood flow (LCBF) in laser Doppler flowmetry (LDF) assay (Fig. 3C). The declined LCBF was maintained

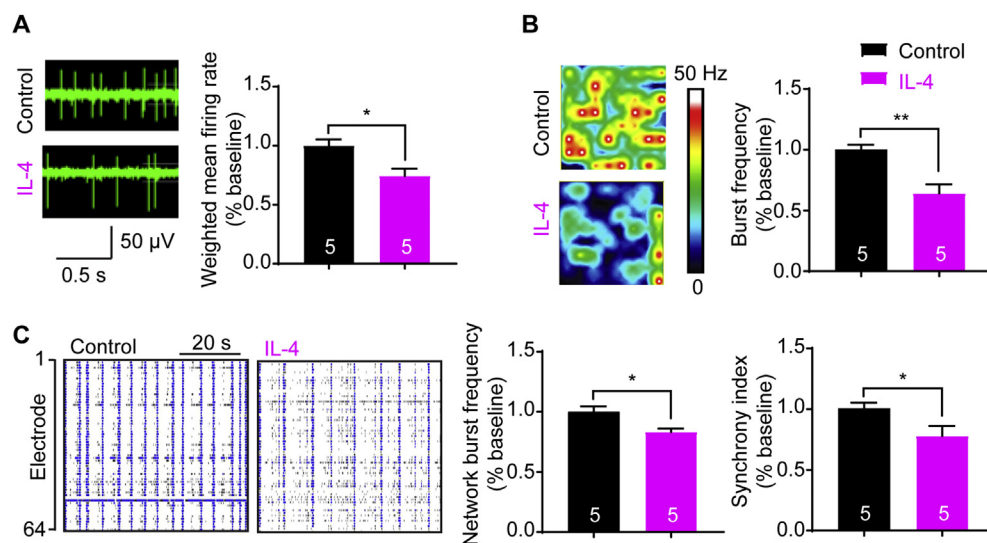


Figure 1 Attenuation of spontaneous firings and network activities of mouse primary cortical neurons by IL-4 in multi-electrode array (MEA) recordings. (A) Raw traces of neuronal firings for a single electrode recordings of mouse primary cortical neurons in the presence or absence of IL-4 (20 ng/mL) after culture of 16 days. (B) Heat-maps of representative MEA recordings of cortical neurons, and reduction of burst frequency in IL-4 group. (C) Well-wide (64 electrodes) raster plots of MEA recordings of cortical neurons for 1.0 min, and reduction of network burst frequency and synchrony index with IL-4. Data are collected from 5 wells of MEA plates (320 electrodes) and are expressed as the mean \pm SEM, * $P < 0.05$ and ** $P < 0.01$ versus the control group. The numbers at the bottom of the bars indicate the number of wells.

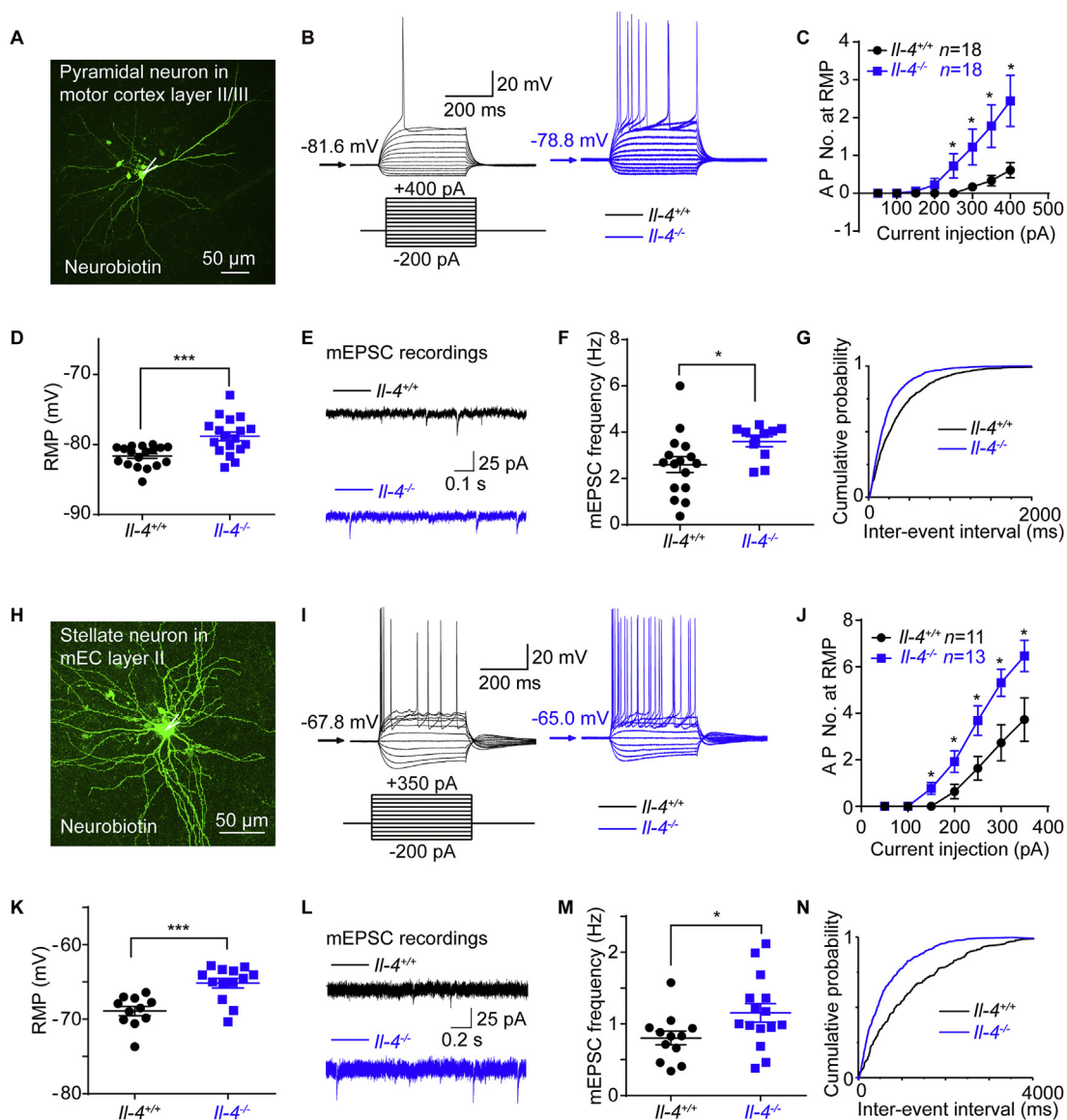


Figure 2 Hyperexcitability and enhanced synaptic transmissions of pyramidal and stellate neurons from *Il-4*^{-/-} mice. (A) Morphology of pyramidal neurons in the motor cortex (M1) layer II/III labeled with neurobiotin. (B) Representative traces for neuronal firings by whole-cell current clamp recordings of *Il-4*^{+/+} and *Il-4*^{-/-} pyramidal neuron. (C) The comparison of fired action potential numbers (AP No.) between of *Il-4*^{-/-} and *Il-4*^{+/+} pyramidal neurons. (D) The resting membrane potentials (RMP) of *Il-4*^{+/+} and *Il-4*^{-/-} pyramidal neurons. (E) Representative traces for miniature excitatory postsynaptic currents (mEPSCs) by voltage-clamp recordings of *Il-4*^{+/+} and *Il-4*^{-/-} pyramidal neurons. (F) Increased frequency of mEPSCs with a cumulative probability of shorter inter-event intervals. (G) In *Il-4*^{-/-} pyramidal neurons. (H) Morphology of a stellate neuron in mEC layer II for patch-clamp recordings. (I) The representative traces for neuronal firings of recordings of *Il-4*^{+/+} and *Il-4*^{-/-} stellate neurons. (J) Comparison of fired AP No. and RMP (K) between of *Il-4*^{+/+} and *Il-4*^{-/-} stellate neurons. (L) Representative traces for mEPSCs in *Il-4*^{+/+} and *Il-4*^{-/-} stellate neurons. (M) Increased frequency of mEPSCs with a cumulative probability of shorter inter-event intervals. (N) in *Il-4*^{-/-} stellate neurons. Data are expressed as the mean \pm SEM; *n* indicates the number of cells recorded, **P* < 0.05, and ****P* < 0.001 versus *Il-4*^{+/+} group.

about 20% of baseline as an indicator for successful occlusion of cerebral blood flow and there are no significant differences of the declined LCBF between the two genotypic groups of mice (Fig. 3C).

For assessment of the cerebral lesion induced by I/R injury, the infarct volume was measured after TTC staining. As shown in Fig. 3D, the total infarct volume of *Il-4*^{-/-} male mice was 2.0-fold larger than those in *Il-4*^{+/+} male mice. The scoring of neurological deficits, determined by an expanded seven-point scale method also revealed that the behavior outcome of *Il-4*^{-/-} male mice (5.00 ± 0.24 , *n* = 10) was significantly worse than that of *Il-4*^{+/+}

mice. Similarly, female *Il-4*^{-/-} mice also exhibited the aggravated behavioral deficits and infarct volume after cerebral I/R injury (Supporting Information Fig. S3).

3.5. *Il-4* deficient neurons are more susceptible to OGD injury and supplementing *IL-4* alleviates OGD injury

To further verify the role of IL-4 in ischemic injury, neurons were subjected to oxygen-glucose deprivation injury for 30 min and reoxygenation (OGD/R) for 24 h (Fig. 4A). Cell death was

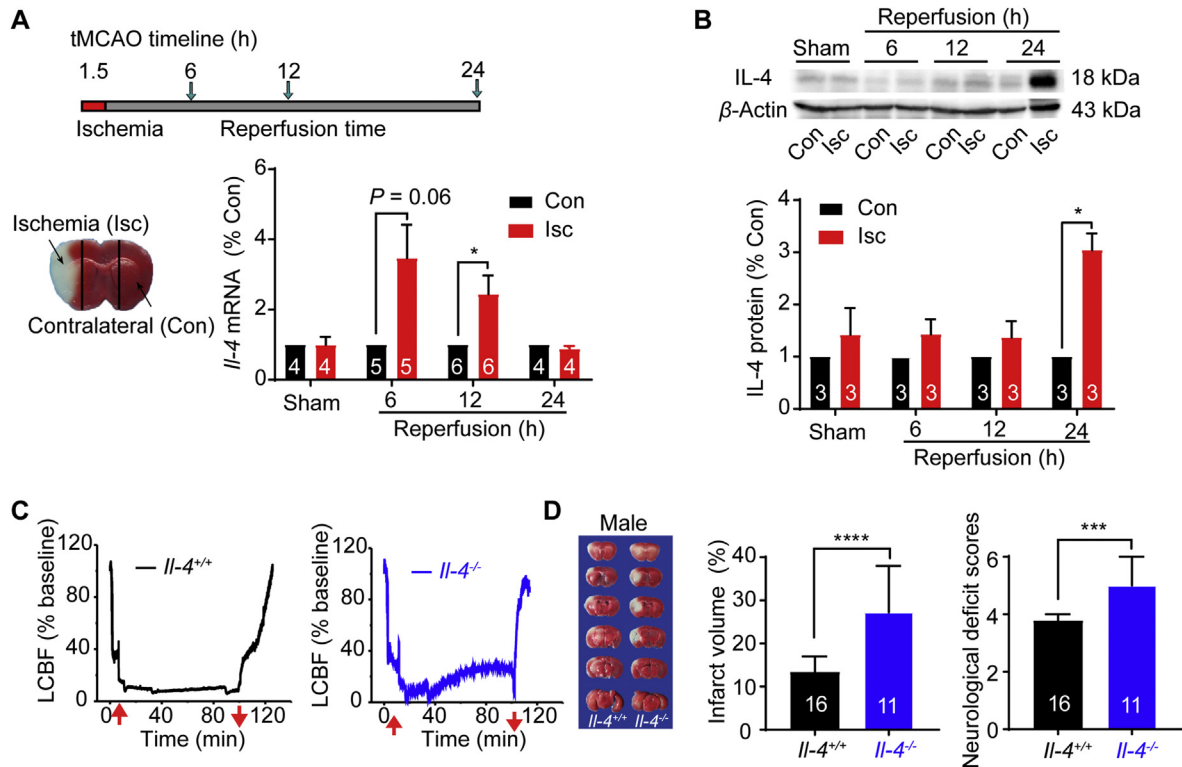


Figure 3 Upregulations of IL-4 after focal ischemia-reperfusion injury and aggravation of brain ischemia by *Il-4* silencing. (A) Schematic timeline of transient middle cerebral artery occlusion (tMCAO) in mice subjected to 1.5 h ischemia before reperfusion for 6, 12 or 24 h, and representative image of ischemic (Isc) and contralateral (Con) regions. Upregulation of *Il-4* mRNA in the Isc region at 6 and 12 h after 1.5 h ischemia by real-time PCR analysis. (B) Upregulation of IL-4 protein expression in Isc at 24 h after reperfusion by Western blot analysis. (C) Representative local cerebral blood flow (LCBF) measured by laser Doppler flowmetry (LDF) in *Il-4*^{+/+} mouse (left) and *Il-4*^{-/-} mouse (right) subject to I/R injury in tMCAO model. Red arrows indicate insertion and withdrawal of the filament. (D) Representative images of TTC-stained brain slices at 24 h after reperfusion from *Il-4*^{+/+} and *Il-4*^{-/-} male mice. The white regions indicate the infarct size, and regions in red indicate the viable tissues. An increase of infarct volume (%) and neurological deficit scores in male *Il-4*^{-/-} mice subjected to I/R injury. Data are presented as the median \pm 95% CI, *** P < 0.001, **** P < 0.0001 versus *Il-4*^{+/+} group for Mann Whitney test. Other data are presented as the mean \pm SEM. The numbers at the bottom of the bars indicate the number of repeats or mice in each group, * P < 0.05, ** P < 0.01, *** P < 0.001.

determined by measuring the lactate dehydrogenase (LDH) release. *Il-4*^{-/-} neurons had an elevated LDH release with approximately 28% more than that in *Il-4*^{+/+} neurons after OGD/R injury (Fig. 4B). Viable cells were measured by CCK-8 assay in which dehydrogenase activity of survival cells is directly proportional to the number of living cells. Data showed that the percentage of viable *Il-4*^{-/-} neurons was about 24% lower than that of *Il-4*^{+/+} neurons subject to OGD/R injury (Fig. 4C), consistent with our earlier *in vivo* data. These results demonstrated that IL-4 deficiency increased the susceptibility of neurons to ischemic injury *in vitro*.

To test any protective effect of IL-4, we added IL-4 (20 ng/mL) in the culture of cortical *Il-4*^{-/-} neurons before subjected to 20 min OGD injury. Supplementing IL-4 resulted in an increased viability of OGD-injured *Il-4*^{-/-} cortical neurons to 144% at 24 h, while at normal condition adding IL-4 had no effect on cell viability of *Il-4*^{-/-} neurons (Fig. 4D–F). These results indicate that adding IL-4 can rescue OGD-induced injury in *Il-4*^{-/-} neurons.

We also tested the neuronal firings in *Il-4*^{-/-} brain slices after incubating 20 ng/mL IL-4 in ACSF for 4 h, and there was no significant difference in neuronal firing between *Il-4*^{-/-} and *Il-4*^{-/-} + IL-4 groups (Supporting Information Fig. S4).

3.6. Upregulation of *Nav1.1* and downregulation of *KCa3.1* and $\alpha 6$ subunit of *GABA_A* receptors in *Il-4*^{-/-} mice and supplemental IL-4 increases *KCa3.1* and $\alpha 6$ subunit mRNA expressions

Neuronal excitability is largely controlled by ion channels in concerted action³⁵. To understand the mechanism underlying the hyperexcitability in *Il-4*^{-/-} mice, we further tested the mRNA expression of ion channels that are critical for neuronal excitability. Among the ion channels tested (Supporting Information Fig. S5), *Nav1.1* mRNA expression was upregulated about 1.2-fold, whereas *KCa3.1* and $\alpha 6$ subunit of *GABA_A* were downregulated to 0.66-fold and 0.78-fold in *Il-4*^{-/-} cortical tissues, respectively (Fig. 5A). Further examination of cultured primary cortical neurons revealed an upregulation of *Nav1.1* mRNA expression about 3.7-fold, and down-regulation of *KCa3.1* and $\alpha 6$ subunit of *GABA_A* to 0.27-fold and 0.24-fold, respectively (Fig. 5B). Western blot analysis further revealed that *Nav1.1* protein expression was increased to 1.5-fold (Fig. 5C), whereas *KCa3.1* and *GABA_A* $\alpha 6$ subunit protein expressions were decreased to 0.19-fold and 0.70-fold in *Il-4*^{-/-} mice, respectively (Fig. 5D and E), consistent with their mRNA expression levels.

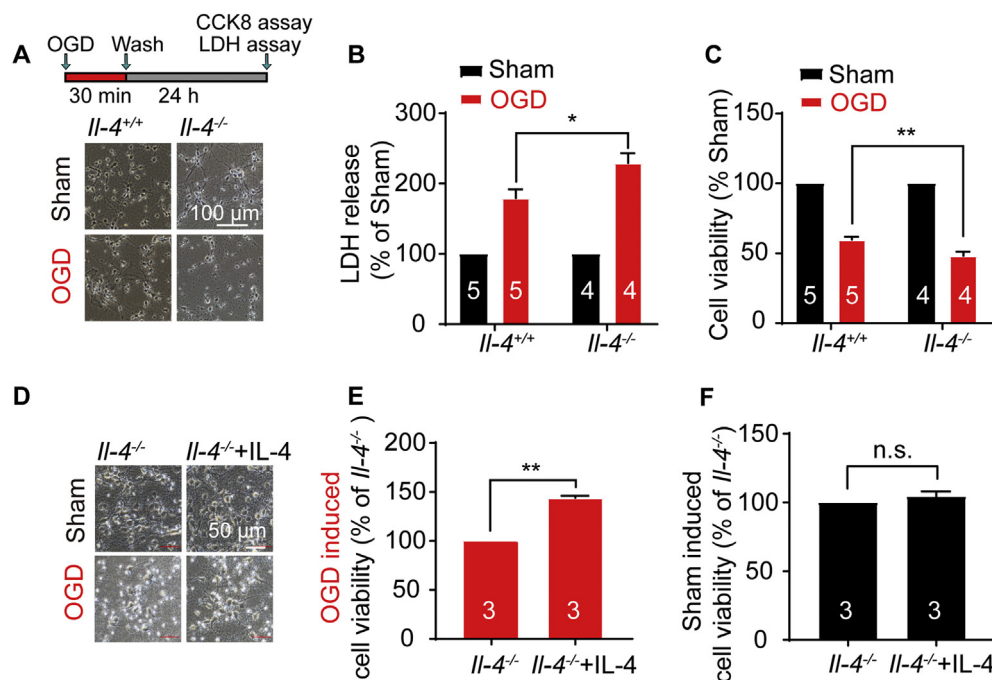


Figure 4 *Il-4* deficient neurons are susceptible to OGD injury and alleviation of the ischemia injury by supplemental IL-4. (A) Cortical neurons were subject to 30 min oxygen-glucose deprivation and 24 h reoxygenation (OGD/R) injury. The representative images for morphological changes of *Il-4*^{+/+} and *Il-4*^{-/-} neurons at 24 h after washout. (B) Increase of the lactate dehydrogenase (LDH) release in LDH assay and (C) decrease of cell viability in Cell Counting Kit-8 (CCK8) assay of *Il-4*^{-/-} primary cortical neurons subject to OGD/R injury. Data are expressed as the mean \pm SEM, *n* indicates the number of mice in each group, **P* < 0.05, ***P* < 0.01 versus *Il-4*^{+/+} group. (D) The representative morphological images of *Il-4*^{-/-} cortical neurons after adding IL-4 (20 ng/mL) for 7 days and subject to 20 min OGD/24 h R injury. Supplementing IL-4 increased the cell viability of *Il-4*^{-/-} cortical neurons in the OGD injury group (E), but not in the Sham group (F). Data are expressed as the mean \pm SEM. The numbers at the bottom of the bars indicate the number of repeats. ***P* < 0.01 versus *Il-4*^{+/+} group, paired student *t*-test. n.s.: no significance.

To test whether supplemental IL-4 could rescue the ion channel expressions, *Il-4*^{-/-} cortical neurons were cultured in the presence of IL-4 (20 ng/mL) or vehicle. RT-PCR analysis showed that the mRNA expressions of *KCa3.1* and $\alpha 6$ subunit increased to 1.6-fold and 4.3-fold, respectively in *Il-4*^{-/-} neurons in the presence of IL-4 compared to vehicle treated *Il-4*^{-/-} neurons (Fig. 5F). In addition, we also tested the effect of supplemental IL-4 on the channel expressions in *Il-4*^{+/+} neurons, and the results showed that the mRNA expressions of *KCa3.1* and $\alpha 6$ subunit were upregulated about 3.6-fold and 4.0-fold respectively in *Il-4*^{+/+} cortical neurons in the presence of IL-4, as compared to vehicle treated *Il-4*^{+/+} neurons (Fig. 5G). These results indicated that neuronal IL-4 deficiency resulted in the upregulation of Nav1.1 and downregulations of both *KCa3.1* and $\alpha 6$ subunit of GABA_A receptors.

4. Discussion

The aim of this study was to test the hypothesis that IL-4 signaling might exert a direct influence on neuronal excitability that defines the fundamental mechanism of brain function and neurological disorders^{18,36}. Our hypothesis was based on the previous investigations that focal ischemia evokes a sudden loss of membrane potentials (anoxic depolarization) in neurons within the ischemic core or ischemic penumbra^{37,38}. The excitotoxicity is

characterized by hyperexcitable neurons and cell death in the absence of oxygen and glucose, which can be reversed by a sodium channel blocker named dibucaine³⁹.

Based on literature findings^{18,40}, IL-4 binds to IL-4R for functioning (Fig. 6). IL-4 deficiency may change gene transcriptions, downregulating *Kcnn4* gene encoding *KCa3.1* protein and *Gabra6* gene encoding GABA_A receptor chloride channel, and upregulating *Scn1a* gene encoding Nav1.1 channel through IL-4 signaling pathways. Downregulation of *KCa3.1* channels reduces potassium outflow, resulting in hyperexcitable with a larger mAHP slope, and decreased tonic GABA_A receptors expression reduces chloride inflow, thus leading to enhanced neuronal firings through membrane depolarization. In addition, the upregulation of Nav1.1 channels can increase sodium inflow into cortical neurons. All these alterations are likely to enhance neuronal excitability and glutamate release from excitatory axonal terminals, ultimately accentuating susceptibility to ischemic injury. Conversely, enhancement of IL-4 signaling through supplemental IL-4 can rescue the expressions of these ion channels, reverse the neuronal excitability and protect against ischemic injury (Fig. 6). These findings support the view that anti-inflammatory IL-4 can protect brains against ischemic injury and promote recovery after ischemic injury^{9,10,41}.

Previous findings have shown that anti-inflammatory cytokines such as IL-4 induce neurogenesis⁴², promote axonal outgrowth to form new connections^{7,43} and modulate synaptic plasticity⁴⁴.

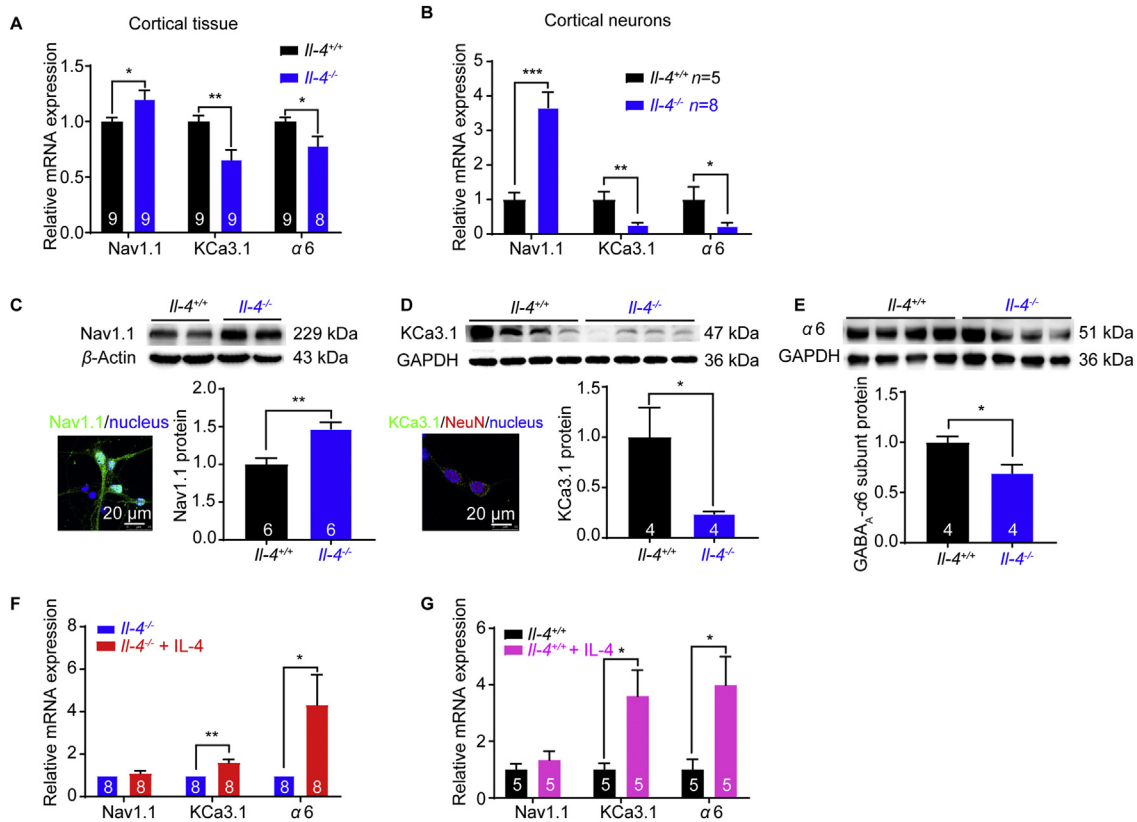


Figure 5 Upregulation of Nav1.1 and downregulations of KCa3.1 and $\alpha 6$ subunit of GABA_A receptors in the cortex from *Il-4*^{-/-} mice and supplemental IL-4 increases *KCa3.1* and $\alpha 6$ mRNA expressions. Upregulation of *Nav1.1* mRNA expression and downregulations of *KCa3.1* and $\alpha 6$ subunit of GABA_A receptors mRNA expression, in cortical tissues (A) and cortical neurons (B) from *Il-4*^{-/-} mice. (C) Nav1.1 protein expression in primary mouse cortical neurons by immunostaining and upregulation of Nav1.1 protein in *Il-4*^{-/-} mice ($n = 6$ mice). (D) The image staining with KCa3.1 antibody (green), NeuN antibody (red, a neuronal-specific nucleus marker) and DAPI (blue, a nucleus marker). Downregulation of KCa3.1 protein in *Il-4*^{-/-} mice ($n = 4$ mice, Mann Whitney test). (E) Downregulation of $\alpha 6$ subunit of GABA_A protein in *Il-4*^{-/-} mice ($n = 4$ mice). Increased mRNA expressions of KCa3.1 and $\alpha 6$ subunit in *Il-4*^{-/-} (F) and *Il-4*^{+/+} (G) cortical neurons after supplementing IL-4 (20 ng/mL) in culture for 7 days. Data are expressed as the mean \pm SEM, * $P < 0.05$, ** $P < 0.01$ and *** $P < 0.001$ compared with their controls. The numbers at the bottom of the bars indicate the number of repeats or mice in the group.

Similar to those findings, our findings reveal IL-4 deficiency leads to repetitive firings, enhanced miniature excitatory transmissions and more susceptibility to ischemic injury, thus supplementing or boosting IL-4 level may decrease neuronal firings and neural network activities, which should be beneficial for functional recovery after ischemic injury. Ion channels are essential for neuronal excitability⁴⁵. In neurons, an excess of sodium influx can reduce membrane potential and lead to cytotoxic edema, and intracellular calcium overload can also trigger a series of pathological events that ultimately result in neuronal apoptosis as well as necrotic death¹. Previous reports demonstrate that IL-4 upregulates KCa3.1, Kv1.3 and Kir2.1 expressions in microglia through IL-4R signaling pathway^{18,46}. IL-4 binding to IL-4R reduces pro-inflammatory cytokine production or alters potassium channel expressions such as KCa3.1, Kv1.3 and Kir2.1 channels that play protective roles in neuroinflammation⁴⁶. KCa3.1 channel also contributes to AHPs in neurons expressing IL-4 receptors¹⁹. Consistent with those investigations, our data show that IL-4 deficiency causes downregulation of KCa3.1 channel and changes of mAHP slope, thus helping lead to increased neuronal excitability.

GABA_A receptors regulate neuronal excitability by local inhibitory controls, which are classified as phasic and tonic inhibitions⁴⁷. Tonic inhibition (*i.e.*, mediated by $\alpha 4$, $\alpha 5$, $\alpha 6$, and δ), but not phasic inhibition (mediated by $\alpha 1$, $\alpha 3$, and $\gamma 2$), induced by GABA_A currents contributes to RMP⁴⁸. Our findings show the downregulation of the tonic $\alpha 6$ subunit, which can be reversed after supplement of IL-4 in both *Il-4*^{-/-} and *Il-4*^{+/+} neurons. The depolarized RMP of *Il-4*^{-/-} neurons is at least partially due to the downregulation of tonic $\alpha 6$ subunit of GABA_A receptors, which is consistent with the observation that IL-1 augments GABA_A receptor function and reduces the excitability of neocortical neurons⁴⁹.

Voltage-gated Nav1.1 channel participates in controlling not only neuronal RMP but also threshold potential^{50,51}. Nav1.1 is mainly expressed in GABAergic inhibitory interneurons rather than excitatory neurons⁵². Under normal physiological conditions, inhibitory GABAergic interneurons are more excitable than excitatory neurons to maintain the balance of neural network excitability⁵³. During or after cerebral ischemia injury, it is likely that the upregulation of Nav1.1 induced by IL-4 deficiency causes GABAergic interneurons hyperexcitable and more susceptible to

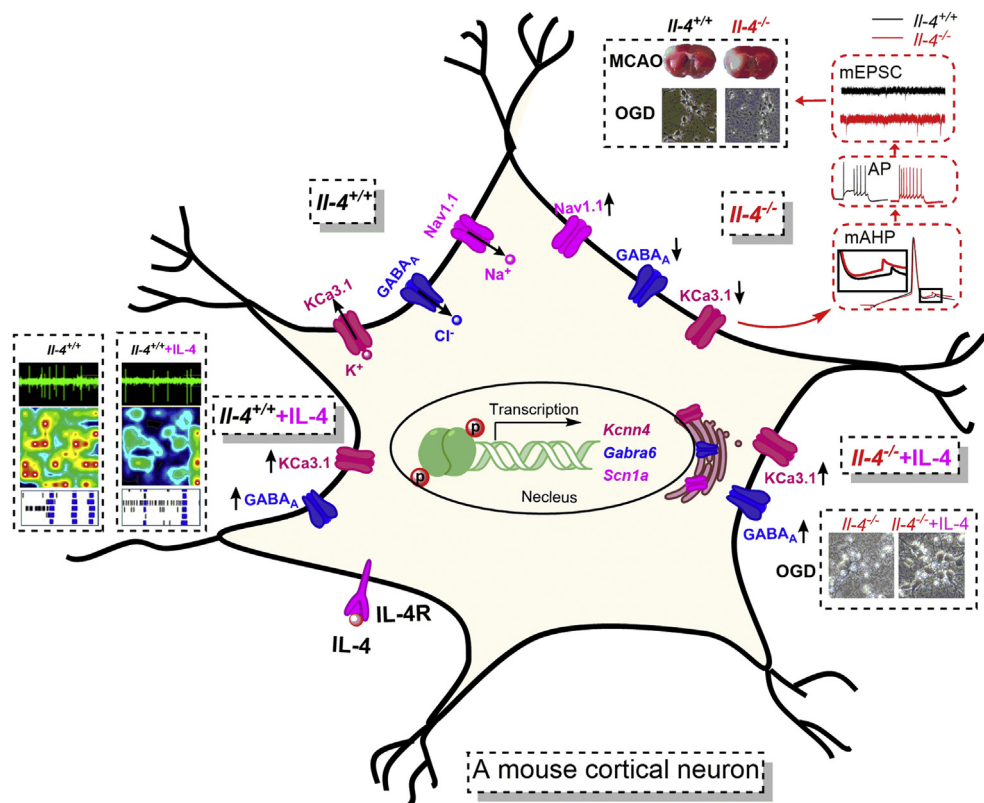


Figure 6 A proposed molecular mechanism underlying increased neural excitabilities and susceptibility to ischemic injury caused by IL-4 deficiency. IL-4 binding to IL-4R activates IL-4 pathway. IL-4 deficiency alters gene transcriptions by downregulating the *Kcnn4* gene encoding KCa3.1 protein and *Gabra6* gene encoding GABA_A receptor chloride channel and upregulating the *Scn1a* gene encoding Nav1.1 protein through IL-4 signaling pathways. Downregulation of KCa3.1 channels and tonic GABA_A receptors can reduce potassium outflow and chloride inflow in neurons, leading to enhanced neuronal firings through membrane depolarization. The upregulation of Nav1.1 channels can increase sodium inflow in neurons. All these alterations can enhance neuronal hyperexcitability and glutamate release from excitatory axon terminals, ultimately increasing susceptibility to ischemic injury. Conversely, enhancement of IL-4 signaling through supplemental IL-4 can increase KCa3.1 and $\alpha 6$ subunit of GABA_A receptors in cortical neurons and reverse neuronal hyperexcitability, thus exerting neuroprotection against ischemic injury.

death than excitatory neurons during ischemia injury. Therefore, the decreased GABA release resulted from a decreased number of GABAergic interneurons will further reduce the inhibitory control over excitatory neurons, causing damage to the balance of network excitability, thus resulting in exacerbation of excitotoxicity.

5. Conclusions

Our findings reveal a previously unknown mechanism by which IL-4 deficiency causes neural hyperexcitability and enhances neuronal excitatory transmissions. IL-4 deficiency leads to an increased vulnerability to ischemic injury. Conversely, supplemental IL-4 reduces neuronal firing and neural network activities, and increases neuronal viability as well. Our data support the view that IL-4 plays a neuroprotective role in ischemia and reperfusion injury. Therefore, supplementing IL-4 might be beneficial for improvement of functional recovery after brain ischemia injury^{6,9–11}.

Acknowledgments

This work was supported by research grants from the National Natural Science Foundation of China (81573410), the National

Science and Technology Major Project (2018ZX09711001-004-006, China) and the Natural Sciences Foundation of Shandong Province (ZR2015QL008, China) awarded to Kewei Wang. Xiaoling Chen is grateful to Chenyu Zhang and Xueqin Jin for the help in Western blot experiments and patch clamp recordings of IL-4 supplementary brain slices, respectively.

Author contributors

Xiaoling Chen and Jingliang Zhang carried out the experiments by collecting and analyzing the data, and also drafted the manuscript. Yan Song and Pan Yang assisted in some experiments. Yang Yang and Zhuo Huang supervised this project. Kewei Wang supervised the project and finalized the manuscript.

Conflicts of interest

All authors declare no conflict of interest in this study.

Appendix A. Supporting information

Supporting data to this article can be found online at <https://doi.org/10.1016/j.apsb.2020.05.002>.

References

- Chen XL, Wang KW. The fate of medications evaluated for ischemic stroke pharmacotherapy over the period 1995–2015. *Acta Pharm Sin B* 2016;**6**:522–30.
- Hossmann KA. Periinfarct depolarizations. *Cerebrovasc Brain Metab Rev* 1996;**8**:195–208.
- Lan X, Han X, Li Q, Yang QW, Wang J. Modulators of microglial activation and polarization after intracerebral haemorrhage. *Nat Rev Neurol* 2017;**13**:420–33.
- Xing CH, Wang XS, Cheng CJ, Montaner J, Mandeville E, Leung W, et al. Neuronal production of lipocalin-2 as a Help-Me signal for glial activation. *Stroke* 2014;**45**:2085–92.
- Han Y, Chen X, Shi F, Li S, Huang J, Xie M, et al. CPG15, a new factor upregulated after ischemic brain injury, contributes to neuronal network re-establishment after glutamate-induced injury. *J Neurotrauma* 2007;**24**:722–31.
- Zhao X, Wang H, Sun G, Zhang J, Edwards NJ, Aronowski J. Neuronal Interleukin-4 as a modulator of microglial pathways and ischemic brain damage. *J Neurosci* 2015;**35**:11281–91.
- Walsh JT, Hendrix S, Boato F, Smirnov I, Zheng J, Lukens JR, et al. MHCII-independent CD4⁺ T cells protect injured CNS neurons via IL-4. *J Clin Invest* 2015;**125**:699–714.
- Lee HK, Koh S, Lo DC, Marchuk DA. Neuronal IL-4/Ralpha modulates neuronal apoptosis and cell viability during the acute phases of cerebral ischemia. *FEBS J* 2018;**285**:2785–98.
- Liu X, Liu J, Zhao S, Zhang H, Cai W, Cai M, et al. Interleukin-4 is essential for microglia/macrophage M2 polarization and long-term recovery after cerebral ischemia. *Stroke* 2016;**47**:498–504.
- Lively S, Hutchings S, Schlichter LC. Molecular and cellular responses to interleukin-4 treatment in a rat model of transient ischemia. *J Neuropathol Exp Neurol* 2016;**75**:1058–71.
- Yang J, Ding S, Huang W, Hu J, Huang S, Zhang Y, et al. Interleukin-4 ameliorates the functional recovery of intracerebral hemorrhage through the alternative activation of microglia/macrophage. *Front Neurosci* 2016;**10**:61.
- Yang R, Lirussi D, Thornton TM, Jolley-Gibbs DM, Diehl SA, Case LK, et al. Mitochondrial Ca²⁺ and membrane potential, an alternative pathway for Interleukin 6 to regulate CD4 cell effector function. *Elife* 2015;**4**:e06376.
- Carey GB, Semenova E, Qi X, Keegan AD. IL-4 protects the B-cell lymphoma cell line CH31 from anti-IgM-induced growth arrest and apoptosis: contribution of the PI-3 kinase/AKT pathway. *Cell Res* 2007;**17**:942–55.
- Zhang JL, Buehner M, Sebald W. Functional epitope of common gamma chain for interleukin-4 binding. *Eur J Biochem* 2002;**269**:1490–9.
- Zhang JL, Simeonowa I, Wang Y, Sebald W. The high-affinity interaction of human IL-4 and the receptor alpha chain is constituted by two independent binding clusters. *J Mol Biol* 2002;**315**:399–407.
- Nagy E, Mocsar G, Sebestyen V, Volko J, Papp F, Toth K, et al. Membrane potential distinctly modulates mobility and signaling of IL-2 and IL-15 receptors in T cells. *Biophys J* 2018;**114**:2473–82.
- Hanley PJ, Musset B, Renigunta V, Limberg SH, Dalpke AH, Sus R, et al. Extracellular ATP induces oscillations of intracellular Ca²⁺ and membrane potential and promotes transcription of IL-6 in macrophages. *Proc Natl Acad Sci U S A* 2004;**101**:9479–84.
- Ferreira R, Lively S, Schlichter LC. IL-4 type 1 receptor signaling upregulates KCNN4 expression, and increases the KCa3.1 current and its contribution to migration of alternative-activated microglia. *Front Cell Neurosci* 2014;**8**:183.
- Nguyen TV, Matsuyama H, Baell J, Hunne B, Fowler CJ, Smith JE, et al. Effects of compounds that influence Ik (KCNN4) channels on after-hyperpolarizing potentials, and determination of Ik channel sequence, in Guinea pig enteric neurons. *J Neurophysiol* 2007;**97**:2024–31.
- Schmitteckert EM, Prokop CM, Hedrich HJ. DNA detection in hair of transgenic mice—a simple technique minimizing the distress on the animals. *Lab Anim* 1999;**33**:385–9.
- Schwieger J, Esser KH, Lenarz T, Scheper V. Establishment of a long-term spiral ganglion neuron culture with reduced glial cell number: effects of AraC on cell composition and neurons. *J Neurosci Methods* 2016;**268**:106–16.
- Yang Y, Adi T, Effraim PR, Chen L, Dib-Hajj SD, Waxman SG. Reverse pharmacogenomics: carbamazepine normalizes activation and attenuates thermal hyperexcitability of sensory neurons due to Nav 1.7 mutation I234T. *Br J Pharmacol* 2018;**175**:2261–71.
- Fogarty MJ, Hammond LA, Kanjhan R, Bellingham MC, Noakes PG. A method for the three-dimensional reconstruction of Neurobiotin-filled neurons and the location of their synaptic inputs. *Front Neural Circ* 2013;**7**:153.
- Zhang J, Chen X, Karbo M, Zhao Y, An L, Wang R, et al. Anticonvulsant effect of dipropofol by enhancing native GABA currents in cortical neurons in mice. *J Neurophysiol* 2018;**120**:1404–14.
- Nunez J. Primary culture of hippocampal neurons from P0 newborn Rats. *JoVE* 2008;(19):895.
- Kopf M, Le Gros G, Bachmann M, Lamers MC, Bluethmann H, Kohler G. Disruption of the murine IL-4 gene blocks Th2 cytokine responses. *Nature* 1993;**362**:245–8.
- Liu F, McCullough LD. The middle cerebral artery occlusion model of transient focal cerebral ischemia. *Methods Mol Biol* 2014;**1135**:81–93.
- Jingliang Zhang TH, Liu Xiaoyan, Zhu Yuanjun, Chen Xiaoling, Liu Ye, Wang Yinze. 002C-3 protects the brain against ischemia-reperfusion injury by inhibiting autophagy and stimulating CaMKK/CaMKIV/HDAC4 pathways in mice. *J Chin Pharmaceut Sci* 2016;**25**:598–604.
- Jackman K, Kunz A, Iadecola C. Modeling focal cerebral ischemia in vivo. *Methods Mol Biol* 2011;**793**:195–209.
- Hu Z, Bian X, Liu X, Zhu Y, Zhang X, Chen S, et al. Honokiol protects brain against ischemia-reperfusion injury in rats through disrupting PSD95–nNOS interaction. *Brain Res* 2013;**1491**:204–12.
- Guan L, Song Y, Gao J, Gao J, Wang K. Inhibition of calcium-activated chloride channel ANO1 suppresses proliferation and induces apoptosis of epithelium originated cancer cells. *Oncotarget* 2016;**7**:78619–30.
- Livak KJ, Schmittgen TD. Analysis of relative gene expression data using real-time quantitative PCR and the 2^{-ΔΔCT} method. *Methods* 2001;**25**:402–8.
- Murphy TH, Corbett D. Plasticity during stroke recovery: from synapse to behaviour. *Nat Rev Neurosci* 2009;**10**:861–72.
- Gloveli T, Schmitz D, Heinemann U. Interaction between superficial layers of the entorhinal cortex and the hippocampus in normal and epileptic temporal lobe. *Epilepsy Res* 1998;**32**:183–93.
- Lai HC, Jan LY. The distribution and targeting of neuronal voltage-gated ion channels. *Nat Rev Neurosci* 2006;**7**:548–62.
- Szucs A, Rubakhin SS, Stefano GB, Hughes TK, Rozsa KS. Interleukin-4 potentiates voltage-activated Ca-currents in *Lymnaea* neurons. *Acta Biol Hung* 1995;**46**:351–62.
- Joshi I, Andrew RD. Imaging anoxic depolarization during ischemia-like conditions in the mouse hemi-brain slice. *J Neurophysiol* 2001;**85**:414–24.
- Bures J, Buresova O. Anoxic terminal depolarization as an indicator of cerebral cortex vulnerability in anoxia & ischemia. *Pflugers Arch für Gesamte Physiol Menschen Tiere* 1957;**264**:325–34.
- Douglas HA, Callaway JK, Sword J, Kirov SA, Andrew RD. Potent inhibition of anoxic depolarization by the sodium channel blocker dibucaine. *J Neurophysiol* 2011;**105**:1482–94.
- Kelly-Welch AE, Hanson EM, Boothby MR, Keegan AD. Interleukin-4 and interleukin-13 signaling connections maps. *Science* 2003;**300**:1527–8.
- Xiong X, Barreto GE, Xu L, Ouyang YB, Xie X, Giffard RG. Increased brain injury and worsened neurological outcome in interleukin-4 knockout mice after transient focal cerebral ischemia. *Stroke* 2011;**42**:2026–32.

42. Butovsky O, Ziv Y, Schwartz A, Landa G, Talpalar AE, Pluchino S, et al. Microglia activated by IL-4 or IFN-gamma differentially induce neurogenesis and oligodendrogenesis from adult stem/progenitor cells. *Mol Cell Neurosci* 2006;**31**:149–60.
43. Vidal PM, Lemmens E, Dooley D, Hendrix S. The role of "anti-inflammatory" cytokines in axon regeneration. *Cytokine Growth Factor Rev* 2013;**24**:1–12.
44. Li Q, Qi F, Yang J, Zhang L, Gu H, Zou J, et al. Neonatal vaccination with bacillus Calmette-Guerin and hepatitis B vaccines modulates hippocampal synaptic plasticity in rats. *J Neuroimmunol* 2015;**288**:1–12.
45. Aldrich R. Molecular biophysics: ionic channels of excitable membranes. *Science* 1985;**228**:867–8.
46. Nguyen HM, Grossinger EM, Horiuchi M, Davis KW, Jin LW, Maezawa I, et al. Differential Kv1.3, KCa3.1, and Kir2.1 expression in "classically" and "alternatively" activated microglia. *Glia* 2017;**65**:106–21.
47. Walker MC, Semyanov A. Regulation of excitability by extrasynaptic GABAA receptors. In: *Darlison MG editor. Inhibitory regulation of excitatory neurotransmission*. Heidelberg: Springer Berlin Heidelberg; 2008. p. 29–48.
48. Lu JC, Hsiao YT, Chiang CW, Wang CT. GABAA receptor-mediated tonic depolarization in developing neural circuits. *Mol Neurobiol* 2014;**49**:702–23.
49. Miller LG, Galpern WR, Dunlap K, Dinarello CA, Turner TJ. Interleukin-1 augments gamma-aminobutyric acidA receptor function in brain. *Mol Pharmacol* 1991;**39**:105–8.
50. Bean BP. The action potential in mammalian central neurons. *Nat Rev Neurosci* 2007;**8**:451–65.
51. Bennett DL, Clark AJ, Huang J, Waxman SG, Dib-Hajj SD. The role of voltage-gated sodium channels in pain signaling. *Physiol Rev* 2019;**99**:1079–151.
52. Lorincz A, Nusser Z. Cell-type-dependent molecular composition of the axon initial segment. *J Neurosci* 2008;**28**:14329–40.
53. Cantu D, Walker K, Andresen L, Taylor-Weiner A, Hampton D, Tesco G, et al. Traumatic brain injury increases cortical glutamate network activity by compromising GABAergic control. *Cerebr Cortex* 2015;**25**:2306–20.